*Bangladesh Journal of Physics, Vol. **33**, Issue 1, pp. 15 – 24, June 2026*

MODELING SURFACE MORPHOLOGY: A FINITE DIFFERENCE STUDY OF COUPLED CONTINUUM EQUATIONS AND THE SCHWOEBEL BARRIER

M. M. ISLAM[1], M. M. RAHMAN[2], AND AIN-UL HUDA[2]

[1]*Department of Computer Science and Engineering, Central Women's University, Dhaka 1203, Bangladesh*
[2]*Department of Physics, Jagannath University, Dhaka 1100, Bangladesh*
Corresponding author: majidurrahman@phy.jnu.ac.bd

Received on 05.01.2026, Revised received on 07.05.2026, Accepted for publication on 15.05.2026

DOI: *https://doi.org/10.3329/bjphy.v33i1.86910*

ABSTRACT

We study coupled continuum equations for surface growth using a finite difference approach, focusing on the interplay between surface diffusion, evaporation–accretion, and the Schwoebel barrier. The growth, roughness, and dynamic exponents are extracted from real-space simulations with and without the Schwoebel barrier. The results are in reasonable agreement with k-space predictions, although finite-size effects lead to a less distinct crossover regime.

Keywords: *k-space computations, Schwoebel barrier, surface diffusion, coupled continuum equations, molecular beam epitaxy, surface growth*

1. INTRODUCTION

The study of surface morphology during growth processes is of fundamental importance in condensed matter physics and materials science, with applications ranging from thin-film deposition to nanostructure formation [1,2]. Surface evolution is governed by competing mechanisms such as atomic diffusion, evaporation–accretion, and interactions with the substrate [3,4]. Surface relaxation and smoothing mechanisms have also been studied in sandpile-type models [5]. A central challenge is to describe the coupled dynamics of mobile and surface-bound atoms, particularly under conditions where substrate heating enhances atomic mobility [6,7].

Recent studies have emphasized the importance of Ehrlich–Schwoebel barriers and surface diffusion in determining nanoscale morphology evolution during epitaxial growth processes [8–15]. Modern investigations combining continuum modeling, atomistic simulations, and molecular beam epitaxy experiments have demonstrated complex pattern formation, step meandering, and diffusion-driven instabilities in thin-film systems.

In this work, we investigate coupled continuum equations describing these processes, incorporating surface diffusion, the Schwoebel barrier, condensation in grooves, and evaporation from mounds. The equations are solved numerically using a finite difference scheme to study the evolution of surface morphology in real space.

We focus on the scaling behavior of the system by computing the growth, roughness, and dynamic exponents, both with and without the Schwoebel barrier. The results are compared with *k*-space

calculations, showing overall agreement, although the crossover regime is less distinct in real-space simulations due to finite-size and averaging effects.

2. METHODOLOGY

Surface growth during molecular beam epitaxy (MBE) can be described at large length scales by a continuum height field $h(x,t)$, which represents the local surface profile relative to the mean height. The dynamics of the surface are governed by stochastic partial differential equations that incorporate surface diffusion, deposition, evaporation–accretion processes, and noise effects [16,17].

In addition to continuum descriptions, discrete growth models such as ballistic deposition have also been extensively studied to understand interface roughening phenomena [18]. These models provide a microscopic basis for deriving coarse-grained continuum equations.

2.1 Governing Growth Equations

The linear surface diffusion process is described by the Mullins–Herring equation [2]:

$$\frac{\partial h}{\partial t} = -K\nabla^4 h + \eta,$$

where *K* is the surface diffusion coefficient and $\eta(x,t)$ represents Gaussian white noise with zero mean. This equation predicts a roughness exponent $\alpha = 3/2$ in one spatial dimension.

2.2 Nonlinear Growth and Renormalization Group Analysis

At larger length scales, nonlinear effects become significant. Imposing mass conservation leads to the conserved nonlinear growth equation:

$$\frac{\partial h}{\partial t} = -K\nabla^4 h + \lambda_1 \nabla^2 (\nabla h)^2 + \eta,$$

where λ_1 represents the strength of nonlinear interactions. Dynamic renormalization group (RG) analysis yields the scaling exponents [19,20]:

$$\alpha = \frac{4-d}{3}, \quad \beta = \frac{4-d}{8+d}, \quad z = \frac{8+d}{3}.$$

For one spatial dimension ($d = 1$), these reduce to:

$$\alpha = 1, \quad \beta = 1/3, \quad z = 3.$$

2.3 Growth with Desorption

The Edwards–Wilkinson (EW) equation describes linear stochastic surface growth dominated by diffusive relaxation and random noise [1]:

$$\frac{\partial h}{\partial t} = \vartheta \nabla^2 h + \eta,$$

where $h(x,t)$ is the surface height, ϑ is the surface relaxation coefficient, and $\eta(x,t)$represents Gaussian white noise. In one spatial dimension, the EW universality class is characterized by:

$$\alpha = \frac{1}{2}, \quad \beta = \frac{1}{4}, \quad z = 2.$$

The Kardar–Parisi–Zhang (KPZ) equation extends the EW equation by including the lowest-order nonlinear growth term $(\nabla h)^2$ [19]:

$$\frac{\partial h}{\partial t} = \vartheta \nabla^2 h + \frac{\lambda}{2}(\nabla h)^2 + \eta.$$

The nonlinear term accounts for lateral growth along the local surface normal and can change the scaling behavior significantly. In one spatial dimension, the KPZ universality class has the exponents

$$\alpha = \frac{1}{2}, \quad \beta = \frac{1}{3}, \quad z = \frac{3}{2}.$$

Thus, the EW equation represents the linear limit of surface relaxation, whereas the KPZ equation describes nonlinear interface growth. In the present study, the generalized growth equation contains both linear relaxation and nonlinear KPZ-type contributions, together with higher-order surface diffusion terms. Therefore, the observed scaling behavior may reflect crossover effects between EW/KPZ-type dynamics and diffusion-dominated conserved growth.

2.4 Coupled Continuum Model

To account for evaporation–accretion and mobile atom dynamics, we employ the coupled continuum model proposed in [6,7]. The system is described by two coupled equations:

$$\frac{\partial h}{\partial t} = -D_h \nabla^4 h - T + \nabla \cdot j_s + \eta_h,$$

$$\frac{\partial \rho}{\partial t} = D_\rho \nabla_2 \rho + T,$$

where $h(x,t)$ is the surface height, $\rho(x,t)$ is the density of mobile atoms, and D_h, D_ρ are diffusion coefficients.

2.5 Schwoebel Barrier and Transfer Term

The Schwoebel barrier is incorporated through an asymmetric surface current:

$$j_s = \frac{D_s m(1-m^2)}{(1-m)^2 + (l_d m)^2}, \qquad m = \frac{dh}{dx}.$$

This term introduces directional bias in atomic diffusion across step edges, resulting in anisotropic mass transport.

The transfer term describing evaporation–accretion is given by:

$$T = \upsilon|\nabla^2 h|[1 - \Theta(\nabla^2 h)] - \mu\rho|\nabla^2 h|\Theta(\nabla^2 h),$$

where $\Theta(x)$ is the Heaviside step function, and $\nabla^2 h$ represents the local surface curvature.

2.6 Numerical Implementation

The governing equations are solved using a finite difference method (FDM) on a one-dimensional lattice (1+1 dimensions). We employ an explicit forward-time central-space (FTCS) scheme with

spatial discretization Δx, and time step Δt. Periodic boundary conditions are imposed to eliminate edge effects. Stability constraints are maintained by ensuring that the time step satisfies the numerical stability condition associated with diffusion-dominated systems.

2.7 Extraction of Scaling Exponents

The surface width is defined as:

$$W(t) = \sqrt{\langle h^2 \rangle - \langle h \rangle^2},$$

The height–height correlation function is given by:

$$C(x) = \langle [h(x + x_0) - h(x_0)]^2 \rangle \sim x^{2\alpha}.$$

The growth exponent β and roughness exponent α are obtained from the slopes of log–log plots, while the dynamic exponent is calculated using:

$$z = \frac{\alpha}{\beta}.$$

3. COMPUTATIONAL DETAILS

The objective of this study is to determine the scaling exponents associated with the coupled continuum equations describing surface growth. The governing equations are solved numerically using a finite difference method (FDM) on a uniform grid in one spatial dimension (1+1). To validate the numerical scheme, we first simulate the Wolf–Villain (WV) model [21], whose scaling properties are well established. Fig. 1 shows the surface profiles at different time steps with diffusion coefficient $D_h = 1.0$. The profiles correspond to 1×10^6 , 2×10^6, and 3×10^6 time steps.

The surface width $W(t)$ is computed for system sizes $N = 500$ and $N = 1000$, averaged over 50 independent configurations (Fig. 2). The results exhibit an initial power-law growth regime followed by saturation, with the crossover time increasing with system size.

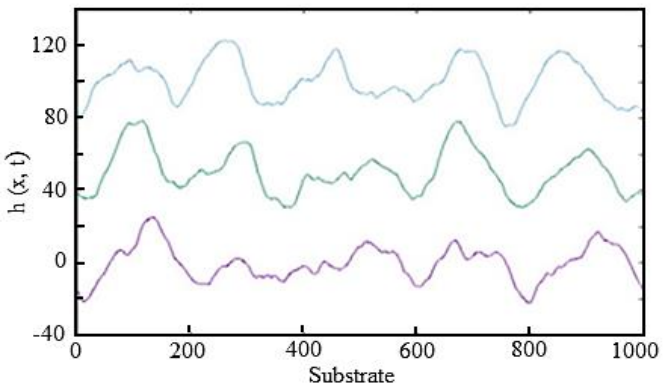

Fig. 1. Surface profile of the Wolf-Villain model in different time steps.

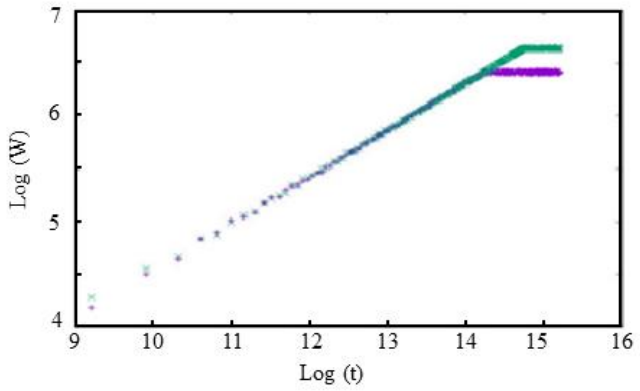

Fig. 2. The width as a function of time for two different substrate sizes (N=500, purple) and (N=1000, green)

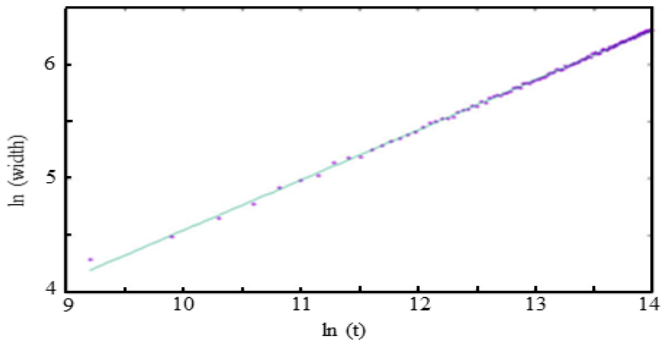

Fig. 3. Log–log plot of the surface width $W(t)$ as a function of time for the Wolf–Villain model. The data are fitted to a straight line with slope $\beta \approx 0.48$, corresponding to the growth exponent.

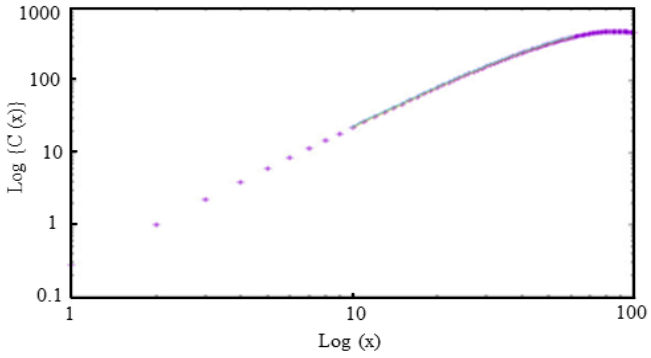

Fig. 4. Log–log plot of the height–height correlation function $C(x)$ as a function of distance x for the Wolf–Villain model. The data follow the scaling relation $C(x) \sim x^{2\alpha}$, yielding a roughness exponent $\alpha = 1.47$.

The growth exponent β is obtained from the slope of the log–log plot of $W(t)$ versus time (Fig. 3), yielding $\beta \approx 0.48$, consistent with theoretical expectations [19,20]. The roughness exponent α is extracted from the height–height correlation function $C(x) \sim x^{2\alpha}$ (Fig. 4), giving $\alpha \approx 1.47$, in agreement with the expected value $\alpha = 3/2$.

Having validated the numerical approach, we simulate the coupled continuum equations. Fig. 5 shows the surface morphology at different times without the Schwoebel barrier, using parameters $D_h = 1.0$, $D_\rho = 1.0$, and $\upsilon = 0.01$.

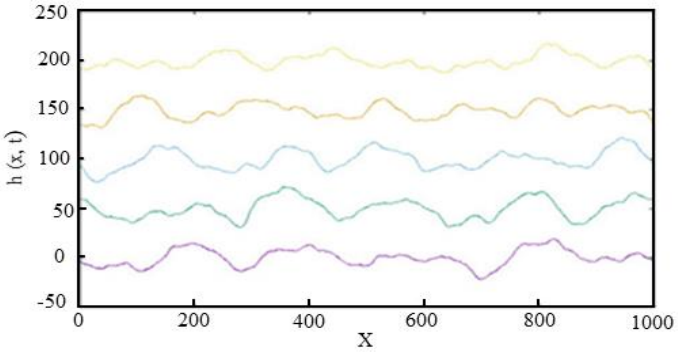

Fig. 5. Surface height profiles obtained from the coupled continuum equation at different time steps.

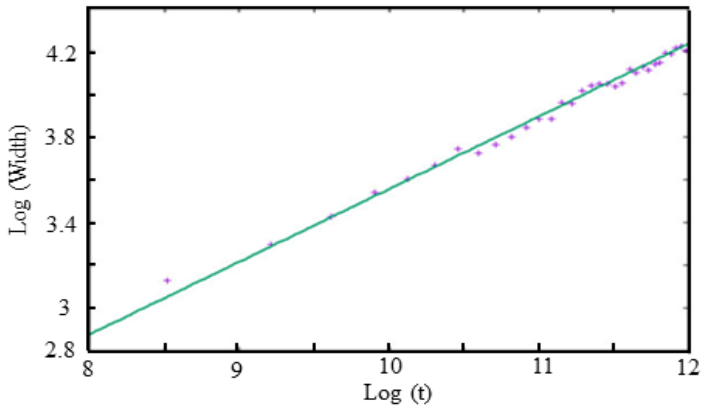

Fig. 6. Log-log plot of the surface width $W(t)$ as a function of time for the coupled continuum equation. The slope of the fitted line yields the growth exponent β.

The growth and roughness exponents are determined from the scaling behavior of the surface width (Fig. 6) and the height–height correlation function (Fig. 7), respectively. The density evolution of mobile atoms is shown in Fig. 8.

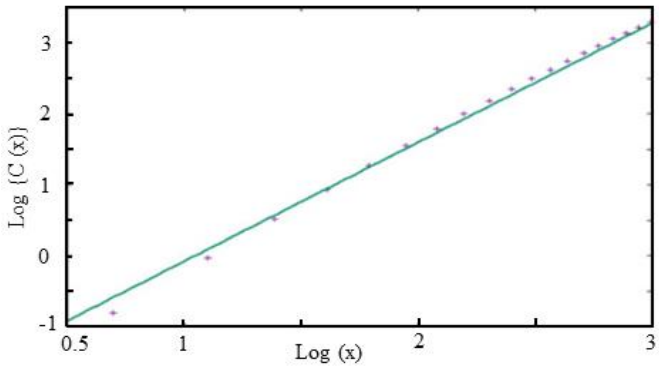

Fig. 7. Log-log plot of the height–height correlation function $C(x)$ as a function of distance x for the coupled continuum equation without the Schwoebel barrier.

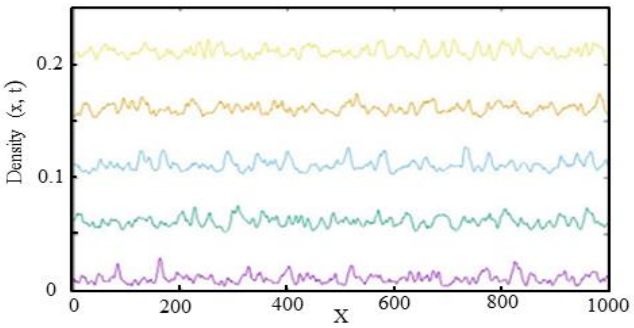

Fig. 8. Density profiles of mobile atoms $\rho(x,t)$ obtained from the coupled continuum equation at different time steps.

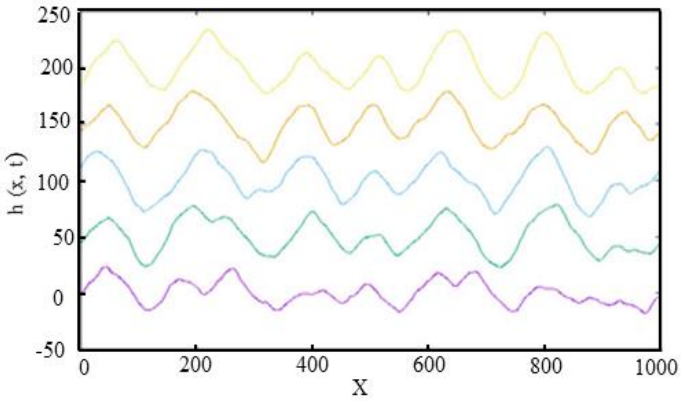

Fig. 9. Surface height profiles obtained from the coupled continuum equation at different time steps in the presence of the Schwoebel barrier.

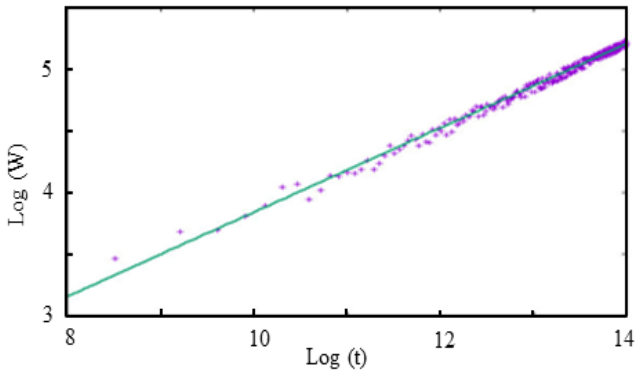

Fig. 10. Log-log plot of the surface width $W(t)$ versus time. The slope gives the growth exponent β.

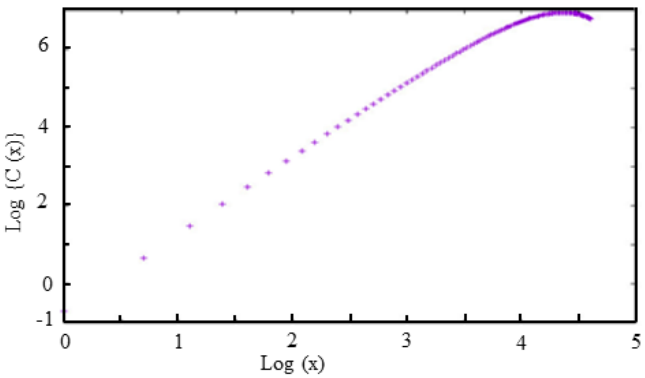

Fig. 11. Log-log plot of the height–height correlation function $C(x)$ as a function of distance x to determine α.

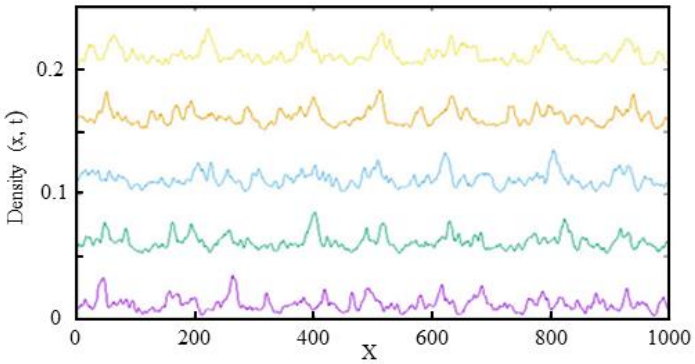

Fig. 12. Density profiles of mobile atoms $\rho(x,t)$ obtained from the coupled continuum equation at different time steps in the presence of the Schwoebel barrier.

We then include the Schwoebel barrier with $l_d = 10$ and repeat the simulations. The corresponding surface profiles are shown in Fig. 9, while the growth and roughness exponents are obtained from Figs. 10 and 11. The evolution of the mobile atom density is shown in Fig. 12.

Table 1. Comparison of growth, roughness, and dynamic exponents obtained from k-space and real-space calculations with and without the Schwoebel barrier.

Exponent	k-space analysis	real-space calculation	k-space (with SB)	real-space (with SB)
Roughness exponent (α)	1.2	1.10	1.36	1.25
Growth exponent (β)	0.36	0.34	0.36	0.32
Dynamic exponent (z)	3.33	3.24	3.78	3.91

The extracted exponents are summarized in Table 1. Compared to k-space calculations, the crossover region in real-space simulations is less pronounced. This discrepancy arises from finite system size, limited simulation time, and reduced configuration averaging. Consequently, the measured exponents should be interpreted as effective exponents, which remain in reasonable agreement with theoretical predictions.

4. CONCLUSIONS

In real-space simulations, the growth (β) and roughness (α) exponents are consistently lower than those obtained from k-space analysis, both with and without the Schwoebel barrier, while the dynamic exponent (z) shows an opposite trend. These differences arise primarily from finite system size ($N = 1000$) and limited configuration averaging (10 realizations), which restrict access to the asymptotic scaling regime. In contrast, k-space calculations typically employ larger system sizes and extensive averaging ($\sim$500 configurations), resulting in more accurate exponent estimates [1, 2, 19, 20].

Acknowledgement

The authors would like to thank the respective authorities for the research fund provided by Jagannath University, Dhaka-1100, Bangladesh.

REFERENCES

[1] A. L. Barabási, H. E. Stanley, *Fractal concepts in surface growth*. Cambridge University Press, 1995.

[2] J. Villain, Continuum models of crystal growth from atomic beams with and without desorption. *Journal de Physique I,* **1**(1), 19–42, 1991.

[3] B. Sanyal, A. Mehta, A. Mookerjee, A new class of coupled continuum equations for atomic growth on surfaces. *Journal of Physics: Condensed Matter,* **11**(22), 4367, 1999.

[4] A. Mookerjee, Growth of rough epitaxial surfaces. *Pramana,* **58**(2), 399–408, 2002.

[5] P. Biswas, S. N. Majumdar, A. Mehta, C. Sire, Smoothing of sandpile surfaces after intermittent and continuous avalanches: Three models in search of an experiment. *Physical Review E,* **58**(2), 1266–1271, 1998.

[6] A. Huda, O. Dutta, A. Mookerjee, Study of a pair of coupled continuum equations modeling surface growth. *International Journal of Modern Physics B,* **17**(16), 2981–2999, 2003.

[7] A. Huda, O. Dutta, A. Mookerjee, Study of a pair of coupled continuum equations modeling surface growth: Interplay between surface diffusion, desorption–accretion and Schwoebel back diffusion. *International Journal of Modern Physics B,* **18**(10–11), 1549–1569, 2004.

[8] M. A. Chabowska, M. A. Załuska-Kotur, Diffusion-dependent pattern formation on crystal surfaces. *ACS Omega*, **8**(48), 45712–45724, 2023.

[9] A. Redkov, Impact of Schwoebel barriers on the step-flow growth of a multicomponent *crystal. Crystals*, **14**(1), 25, 2024.

[10] M. A. Chabowska, H. Popova, M. A. Załuska-Kotur, Step meandering: The balance between the potential well and the Ehrlich–Schwoebel barrier. *Physical Review B*, **111**, 155401, 2025.

[11] Y. Zhang et al. Van der Waals epitaxial growth of single-crystal molecular film. National *Science Review*, **11**(11), 2024.

[12] P. De Padova et al., The role of SiO_2 buffer layer in the molecular beam epitaxy growth of $CsPbBr_3$ perovskite on Si (111). *Scientific Reports*, **14**, 23618, 2024.

[13] K. Choudhary, B. Jalan, Atomically precise synthesis of oxides with hybrid molecular beam epitaxy, 2025.

[14] X. Li, Y. Wang, Z. Chen, Numerical investigation of nonlinear surface evolution equations in epitaxial thin-film growth. *Applied Surface Science*, **605**, 154716, 2022.

[15] H. Sun, Q. Liu, Y. Zaho, Continuum modeling and dynamic scaling analysis of epitaxial surface growth with surface diffusion. *Surface Science Reports*, **78**(4), 2023.

[16] A. Pimpinelli, J. Villain, *Physics of crystal growth*. Cambridge University Press, 1998.

[17] M.A. Makeev, A. L. Barabási, Effect of surface morphology on sputtering yields: I. Ion sputtering from self-affine surfaces. *Nuclear Instruments and Methods in Physics Research Section B,* **222**(3–4), 316–334, 2004.

[18] R. M. D'Souza, Anomalies in simulations of nearest neighbor ballistic deposition. *International Journal of Modern Physics C,* **8**(4), 941–951, 1997.

[19] M. Kardar, G. Parisi, Y. C. Zhang, Dynamic scaling of growing interfaces. *Physical Review Letters,* **56**(9), 889–892, 1986.

[20] S. Pal, D. P. Landau, (1999). The Edwards–Wilkinson model revisited: Large-scale simulations of dynamic scaling in 2+1 dimensions. *Physica A: Statistical Mechanics and Its Applications,* **267**(3–4), 406–413, 1999.

[21] Z. Xun, G. Tang, K. Han, H. Xia, D. Hao, X. Yang, W. Zhou, Extensive numerical study of the anomalous dynamic scaling of the Wolf–Villain model. *Physica A: Statistical Mechanics and Its Applications,* **389**, 2189–2196, 2010.